

Projected Sensivity to Dimension-6 Triple Gauge Couplings at the FCC-hh

V. Ari,^{1,*} V. Cetinkaya,^{2,†} M. Köksal,^{3,‡} and O. Cakir^{4,§}

¹*Department of Physics, Ankara University, 06100, Ankara, Turkey*

²*Department of Physics, Kütahya Dumlupınar University, 43100, Kütahya, Turkey*

³*Department of Physics, Sivas Cumhuriyet University, 58140, Sivas, Turkey*

⁴*Department of Physics, Ankara University, 06100 Ankara, Turkey*

Abstract

In this study, we investigate the process $pp \rightarrow W^\pm \gamma$ for the physics potential of the FCC-hh with $\sqrt{s} = 100$ TeV to examine the anomalous $WW\gamma$ couplings defined by three CP-conserving and two CP-violating effective operators of dimension-6. The analysis containing the realistic detector effects is carried out in the mode where W^\pm bosons in the final state decay into the leptonic channel. The best sensitivities obtained from the process $pp \rightarrow W^\pm \gamma$ on the anomalous couplings C_{WWW}/Λ^2 and $C_{W,B}/\Lambda^2$ determined by CP-conserving effective Lagrangians are $[-0.01; 0.01]$ TeV⁻² and $[-0.88; 0.88]$ TeV⁻², while $C_{\tilde{W}WW}/\Lambda^2$ and $C_{\tilde{W}}/\Lambda^2$ couplings defined by CP-violating effective Lagrangian are obtained as $[-0.03; 0.03]$ TeV⁻² and $[-0.47; 0.47]$ TeV⁻² at the FCC-hh with $\sqrt{s} = 100$ TeV, $L_{int} = 30$ ab⁻¹. However, if the systematic uncertainty is included, we obtain reduced sensitivities on the anomalous $WW\gamma$ coupling. The results are compared for assumed systematics of 5% and 10%.

*vari@science.ankara.edu.tr

†volkan.cetinkaya@dpu.edu.tr

‡mkoksal@cumhuriyet.edu.tr

§ocakir@science.ankara.edu.tr

I. INTRODUCTION

Gauge boson self-interactions are exactly described by the non-abelian gauge symmetry of the Standard Model (SM). These interactions are important for understanding the gauge structure of the SM and new physics studies beyond the SM. Any deviations from the SM predictions on gauge boson self-interactions such as triple gauge boson couplings can give us important information related to the existence of new physics beyond the SM. To probe possible deviations on the triple gauge boson couplings arising from new physics in a model-independent way using the effective Lagrangian method is ordinarily a usual way. The effective Lagrangian including the higher operators than dimension-4 is given as follows

$$\mathcal{L}_{eff} = \mathcal{L}_{SM} + \sum_{D>4} \sum_i \frac{C_i^D}{\Lambda^{D-4}} \mathcal{O}_i^{(D)}. \quad (1)$$

Here, C_i shows the coefficients of the dimension-D operator, Λ is the new physics scale, \mathcal{O}_i is the desired operators. Avoiding the lepton and baryon number violation the effective Lagrangian becomes [1]

$$\mathcal{L}_{eff} = \mathcal{L}_{SM} + \sum_i \frac{C_i^6}{\Lambda^2} \mathcal{O}_i^{(6)} + \sum_i \frac{C_i^8}{\Lambda^4} \mathcal{O}_i^{(8)} + \dots \quad (2)$$

which includes only the even order effective operators. It is easily seen from the above equation that if we want to examine the effects of dimension-D operators ($D = 6, 8, \dots$) at low energies, it gradually decreases.

As known, the kinetic terms of the gauge fields in the SM produce the interactions of triple WWZ and $WW\gamma$ gauge bosons at the tree-level due to the non-abelian nature of $SU(2)_L$ symmetry. However, there are no neutral triple ZZZ , $ZZ\gamma$, $Z\gamma\gamma$ and $\gamma\gamma\gamma$ gauge couplings at the tree-level in the SM. On the other hand, as mentioned above, the effective higher dimension operators may induce and modify the triple gauge boson interactions in the SM. To the lowest order (dimension-6), the operators contributing to WWZ and $WW\gamma$ couplings, respecting the SM gauge symmetry, are [2–4]

$$\mathcal{O}_{WWW} = \text{Tr} [W_{\mu\nu} W^{\nu\rho} W_{\rho}^{\mu}] , \quad (3)$$

$$\mathcal{O}_W = (D_{\mu}\Phi)^{\dagger} W^{\mu\nu} (D_{\nu}\Phi) , \quad (4)$$

$$\mathcal{O}_B = (D_\mu \Phi)^\dagger B^{\mu\nu} (D_\nu \Phi) , \quad (5)$$

$$\mathcal{O}_{\tilde{W}WW} = \text{Tr} \left[\tilde{W}_{\mu\nu} W^{\nu\rho} W_\rho^\mu \right] , \quad (6)$$

$$\mathcal{O}_{\tilde{W}} = (D_\mu \Phi)^\dagger \tilde{W}^{\mu\nu} (D_\nu \Phi) , \quad (7)$$

where Φ represents the Higgs doublet field. D_μ , $W_{\mu\nu}$ and $B_{\mu\nu}$ are defined as

$$D_\mu \equiv \partial_\mu + i \frac{g'}{2} B_\mu + i g W_\mu^i \frac{\tau^i}{2} , \quad (8)$$

$$W_{\mu\nu} = \frac{i}{2} g \tau^i (\partial_\mu W_\nu^i - \partial_\nu W_\mu^i + g \epsilon_{ijk} W_\mu^j W_\nu^k) , \quad (9)$$

and

$$B_{\mu\nu} = \frac{i}{2} g' (\partial_\mu B_\nu - \partial_\nu B_\mu) . \quad (10)$$

Here, τ^i shows the $SU(2)_I$ generators with $\text{Tr} [\tau^i \tau^j] = 2\delta^{ij}$ ($i, j = 1, 2, 3$). The g and g' are $SU(2)_I$ and $U(1)_Y$ couplings, respectively.

The operators in Eqs. (3-7) are invariant under $SU(2)_I \otimes U(1)_Y$ gauge symmetry. To establish SM couplings or to capture new physics beyond the SM regardless of any symmetry, one has to go beyond the SM gauge symmetry. Therefore, one can simply think the Lorentz invariance and $U(1)$ symmetry to establish more general form factors as a function of the momentum concerned in a given vertex. In the form factor formalism, the effective Lagrangian for $WW\gamma$ interaction can be given by [5]

$$\begin{aligned} \mathcal{L}_{WW\gamma} = & ig_{WW\gamma} \left[g_1^\gamma (W_{\mu\nu}^+ W_\mu^- A_\nu - W_{\mu\nu}^- W_\mu^+ A_\nu) \right. \\ & + \kappa_\gamma W_\mu^+ W_\nu^- A_{\mu\nu} + \frac{\lambda_\gamma}{M_W^2} W_{\mu\nu}^+ W_{\nu\rho}^- A_{\rho\mu} \\ & + ig_4^\gamma W_\mu^+ W_\nu^- (\partial_\mu A_\nu + \partial_\nu A_\mu) \\ & - ig_5^\gamma \epsilon_{\mu\nu\rho\sigma} (W_\mu^+ \partial_\rho W_\nu^- - \partial_\rho W_\mu^+ W_\nu^-) A_\sigma \\ & \left. + \tilde{\kappa}_\gamma W_\mu^+ W_\nu^- \tilde{A}_{\mu\nu} + \frac{\tilde{\lambda}_\gamma}{M_W^2} W_{\lambda\mu}^+ W_{\mu\nu}^- \tilde{A}_{\nu\lambda} \right] , \end{aligned} \quad (11)$$

where $g_{WW\gamma} = -e$ and $\tilde{A}_{\mu\nu} = \frac{1}{2}\epsilon_{\mu\nu\rho\sigma}A^{\rho\sigma}$. Here, $A^{\mu\nu} = \partial^\mu A^\nu - \partial^\nu A^\mu$ is the field strength tensor for photon. In above equation, g_1^γ , κ_γ and λ_γ anomalous parameters are both C and P conserving while g_4^γ , g_5^γ , $\tilde{\kappa}_\gamma$ and $\tilde{\lambda}_\gamma$ anomalous parameters are C and/or P violating. The anomalous couplings are described by $\Delta\kappa_\gamma = \lambda_\gamma = 0$ ($\Delta\kappa_\gamma = \kappa_\gamma - 1$) at the tree-level in the SM. Nevertheless, CP-violating interactions can be confined separately to specially designed CP-odd observables that are insensitive to CP-even effects. For this reason, the CP-violating and CP-conserving interactions can be distinguished from each other. In this case, κ_γ and λ_γ couplings can be transformed into c_{WWW}/Λ^2 , c_W/Λ^2 and c_B/Λ^2 couplings as follows [4]

$$\kappa_\gamma = 1 + (c_W + c_B) \frac{m_W^2}{2\Lambda^2}, \quad (12)$$

$$\lambda_\gamma = c_{WWW} \frac{3g^2 m_W^2}{2\Lambda^2}, \quad (13)$$

$$\tilde{\kappa}_\gamma = c_{\tilde{W}} \frac{m_W^2}{2\Lambda^2}, \quad (14)$$

$$\tilde{\lambda}_\gamma = c_{\tilde{W}WW} \frac{3g^2 m_W^2}{2\Lambda^2}. \quad (15)$$

Here, c_{WWW}/Λ^2 , c_W/Λ^2 and c_B/Λ^2 couplings represent the possible deviations for $WW\gamma$ vertex in the SM. These parameters are equal to zero in the SM.

Many studies in the literature that theoretically include the anomalous $WW\gamma$ and WWZ couplings [6–34]. The anomalous $WW\gamma$ couplings have been also studied experimentally at the LEP [35–37], the Tevatron [38–41] and the LHC [42–45]. In Table I, the best limits are given at 95% C.L. on $c_{\tilde{W}WW}/\Lambda^2$, c_{WWW}/Λ^2 , $c_{\tilde{W}}/\Lambda^2$, c_W/Λ^2 and c_B/Λ^2 parameters obtained from the experiments.

After the completion of the LHC and high center-of-mass energy and luminosity LHC physics programs, the future circular collider projects that are the FCC-ee, the FCC-eh and the FCC-hh are proposed to precisely measure the electroweak symmetry breaking mechanism of the SM and new physics effects beyond the SM. Triple Gauge Couplings (TGCs) have been studied [46–48] at future colliders. Among these colliders, the FCC-hh has an energy scale that increases by about 7 times depending on the process compared to the LHC, and in this respect it is also very important for new physics studies, for example the

TABLE I: The best limits at 95% Confidence Level (C.L.) on $c_{\tilde{W}WW}/\Lambda^2$, $c_{W\tilde{W}W}/\Lambda^2$, c_W/Λ^2 , c_B/Λ^2 and $c_{\tilde{W}}/\Lambda^2$ parameters obtained from the LHC experiments.

Experimental limit	$c_{\tilde{W}WW}/\Lambda^2$ (TeV ⁻²)	$c_{W\tilde{W}W}/\Lambda^2$ (TeV ⁻²)	c_W/Λ^2 (TeV ⁻²)	c_B/Λ^2 (TeV ⁻²)	$c_{\tilde{W}}/\Lambda^2$ (TeV ⁻²)
ATLAS [43]	[-5.30; 5.30]	—	[-6.40; 11.0]	[-36.0; 43.0]	—
($WW/WZ \rightarrow l\nu_l qq'$)					
($\sqrt{s} = 8$ TeV and $L_{int} = 20.2$ fb ⁻¹)					
CMS [44]	—	[-5.70; 5.90]	[-11.4; 5.40]	[-29.2; 23.9]	—
($\sqrt{s} = 8$ TeV and $L_{int} = 19.4$ fb ⁻¹)					
CMS [45]	—	[-1.58; 1.59]	[-2.00; 2.65]	[-8.78; 8.54]	—
($\sqrt{s} = 13$ TeV and $L_{int} = 35.9$ fb ⁻¹)					
CMS [49]	[-0.90; 0.91]	[-0.45; 0.45]	[-39.7; 40.7]	[-39.7; 40.7]	[-20.3; 20.0]
($W\gamma \rightarrow l\nu_l\gamma$)					
($\sqrt{s} = 13$ TeV and $L_{int} = 137$ fb ⁻¹)					

anomalous trilinear gauge boson couplings. The FCC-hh is planned to reach an integrated luminosity of 30 ab⁻¹ at a center-of-mass energy of 100 TeV [50].

The rest of our study is organized as follows: In Section II, we will present the production of the signal and the background events of the process $pp \rightarrow W^\pm\gamma$ at the FCC-hh. The limits on the anomalous couplings will be obtained in Section III. Finally, we conclude with the sensitivities of each anomalous coupling discussed in Section IV.

II. PRODUCTION OF SIGNAL AND BACKGROUND EVENTS

The effects of the anomalous contributions arising from dimension-6 operators and SM contributions as well as interference between new physics and the SM contribution are performed via the process $pp \rightarrow W^\pm\gamma$ at the FCC-hh. For this purpose, the tree-level Feynman diagrams of the process $pp \rightarrow W^\pm\gamma$ are given in Fig.1. In this figure, the first diagram comprises the anomalous $WW\gamma$ couplings and the others come from the SM processes. In order to investigate the effects of the anomalous couplings on the process $pp \rightarrow W^\pm\gamma$, we use MadGraph5-aMC@NLO [51] after implementation of the operators Eqs.(3)–(7) through

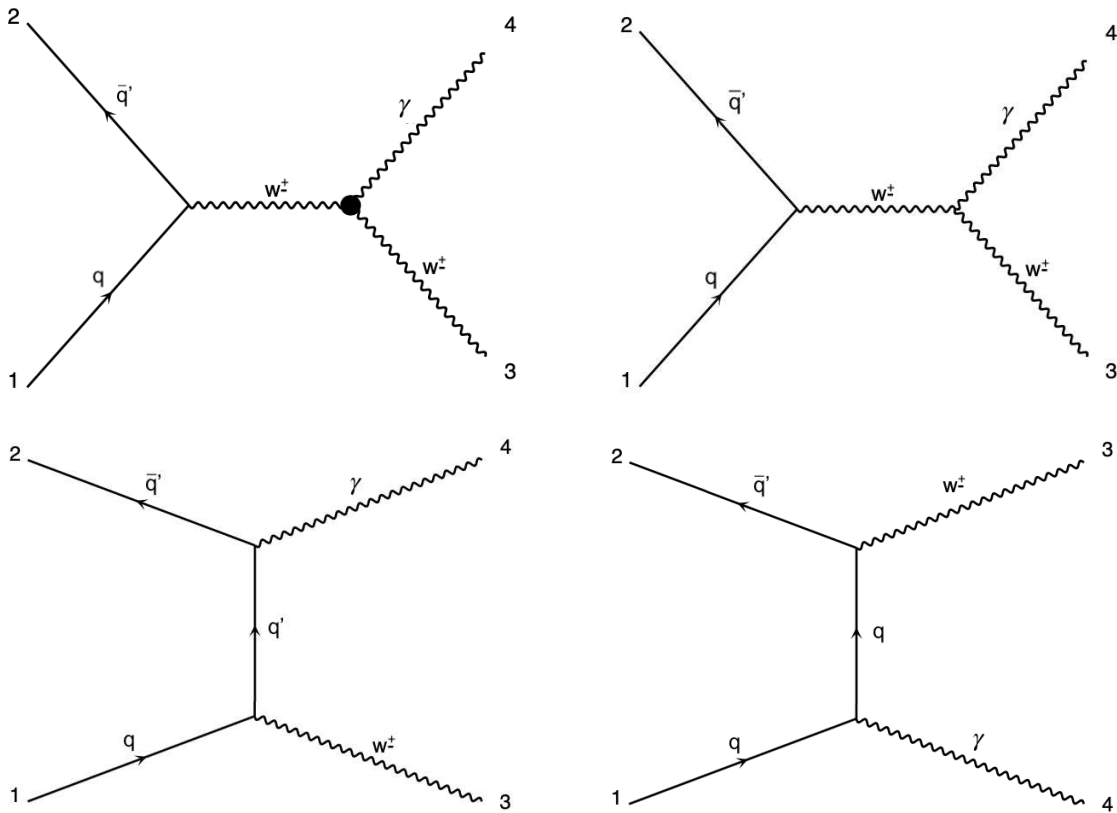


FIG. 1: Feynman diagrams for the subprocess $q\bar{q} \rightarrow W^\pm \gamma$ including the effective $WW\gamma$ vertex.

Feynrules package [52] as a Universal FeynRules Output (UFO) module [53]. The generated signal and relevant backgrounds in MadGraph5–aMC@NLO are passed through Pythia 8 for parton shower and hadronization [54]. The detector responses are taken into account with Delphes package [55]. We have used Delphes default parameters with the FCC-hh card for the detector simulation. However, all events are analyzed using the ExRootAnalysis utility [56] with ROOT [57].

In this work, we examine the anomalous $WW\gamma$ couplings through the process $pp \rightarrow W^\pm \gamma \rightarrow \ell^\pm \nu_\ell (\bar{\nu}_\ell) \gamma$ ($\ell^\pm = e^\pm, \mu^\pm$) at the FCC-hh. Here, the final state topology of the investigated process occurs a photon, a charged lepton and missing energy. Thus, as backgrounds, the following relevant SM background processes having the same or similar final state topology are taken into consideration;

$$SM : pp \rightarrow \ell^\pm \nu_\ell (\bar{\nu}_\ell) \gamma, \quad (16)$$

$$Z + \gamma : pp \rightarrow Z \gamma, \quad (17)$$

$$W + j : pp \rightarrow W^\pm j, \quad (18)$$

$$W + W + \gamma : pp \rightarrow W^\pm W^\mp \gamma, \quad (19)$$

$$W + Z + \gamma : pp \rightarrow W^\pm Z \gamma, \quad (20)$$

$$W + j + \gamma : pp \rightarrow W^\pm j \gamma, \quad (21)$$

$$Z + j + \gamma : pp \rightarrow Z j \gamma, \quad (22)$$

$$W + 2j + \gamma : pp \rightarrow W^\pm jj \gamma, \quad (23)$$

$$Z + Z + \gamma : pp \rightarrow ZZ \gamma. \quad (24)$$

We generate $W\gamma + jets$ and $Z\gamma + jets$ events with MG5 at the leading order. We apply a high p_T cut on the photon, then extra photons will be suppressed. For the preselection and kinematical cuts of leptons, photon and jets included in some backgrounds for the signal and the relevant backgrounds, we apply a minimum cuts (generator level):

- $p_T^l > 10$ GeV, $p_T^j > 20$ GeV, $p_T^\gamma > 100$ GeV,
- $|\eta^l| < 2.5$, $|\eta^j| < 5$, $|\eta^\gamma| < 2.5$,
- $\Delta R(\gamma, \ell) > 0.4$, $\Delta R(\gamma, j) > 0.4$, $\Delta R(\ell, j) > 0.4$.

Here, while $p_T^{l,j,\gamma}$ are the transverse momenta of the final state particles, $\eta^{l,j,\gamma}$ are the pseudorapidities of the final state particles. To have well-separated charged leptons, jets and the photon in the phase space, we require angular separations ($\Delta R = ((\Delta\phi)^2 + (\Delta\eta)^2)^{1/2}$). Actually, we do not require extra jets on the signal selection, however, in the background generation we allow at most one jet. We have not considered fake signal from the conversion jets to electrons or photons.

In Figs. 2 and 3, the total cross-sections of the process $pp \rightarrow W^\pm \gamma$ as a function of the anomalous $C_{\tilde{W}}/\Lambda^2$, C_W/Λ^2 , C_B/Λ^2 , $C_{\tilde{W}WW}/\Lambda^2$ and C_{WWW}/Λ^2 couplings are given. Here, one of the anomalous couplings is non-zero at any time, while the other couplings are fixed to

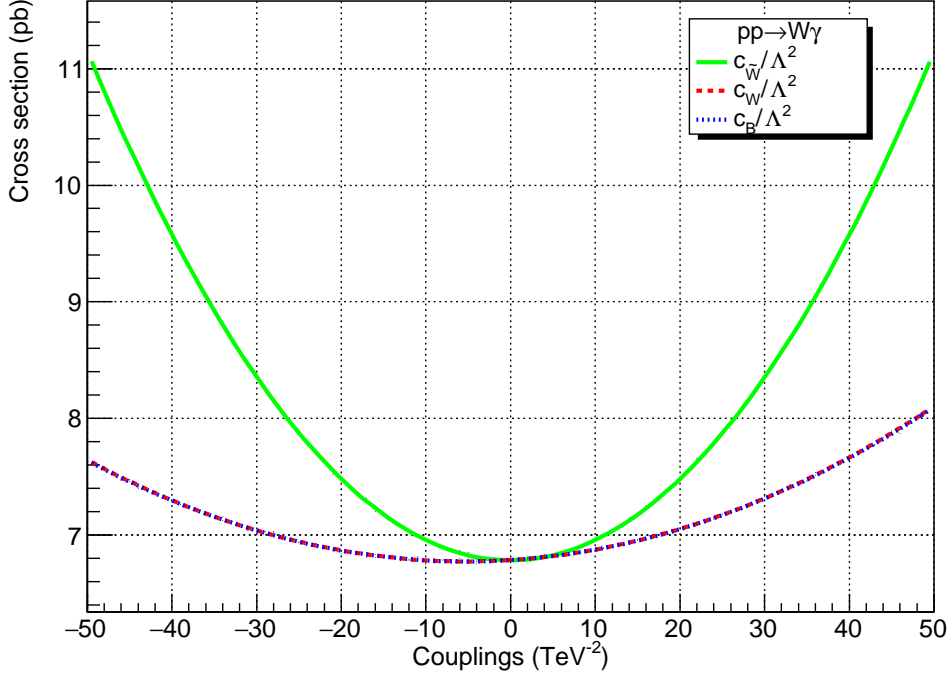


FIG. 2: The total cross-sections of the process $pp \rightarrow W^\pm \gamma$ as a function of the anomalous $C_{\tilde{W}}/\Lambda^2$, C_W/Λ^2 and C_B/Λ^2 couplings at the FCC-hh.

zero. As can be seen from Figs. 2 and 3, the total cross-sections of the process $pp \rightarrow W^\pm \gamma$ increase with increasing coupling values. For C_W/Λ^2 and C_B/Λ^2 , we obtain degenerate behavior of the cross sections as seen in Fig. 2. The cross-sections after using the minimal cut set are given in Table II to show the effects of the signal and the relevant backgrounds for different values of the anomalous couplings. In this table, the cross-sections for the signal and the backgrounds in the relevant mode and decay channel are given. The final state topology of the signal is characterized as a high p_T^γ associated with a lepton and missing transverse momentum from the undetected neutrino. We also take into account the final states associated with a photon as background in the event generation and account for the detector responses in the simulation.

Thus, in order to distinguish signal from relevant backgrounds, we also apply the following analysis cuts:

- $N_\ell \geq 1, N_\gamma \geq 1$,
- $p_T^l > 35 \text{ GeV}, |\eta^l| < 2.5$,

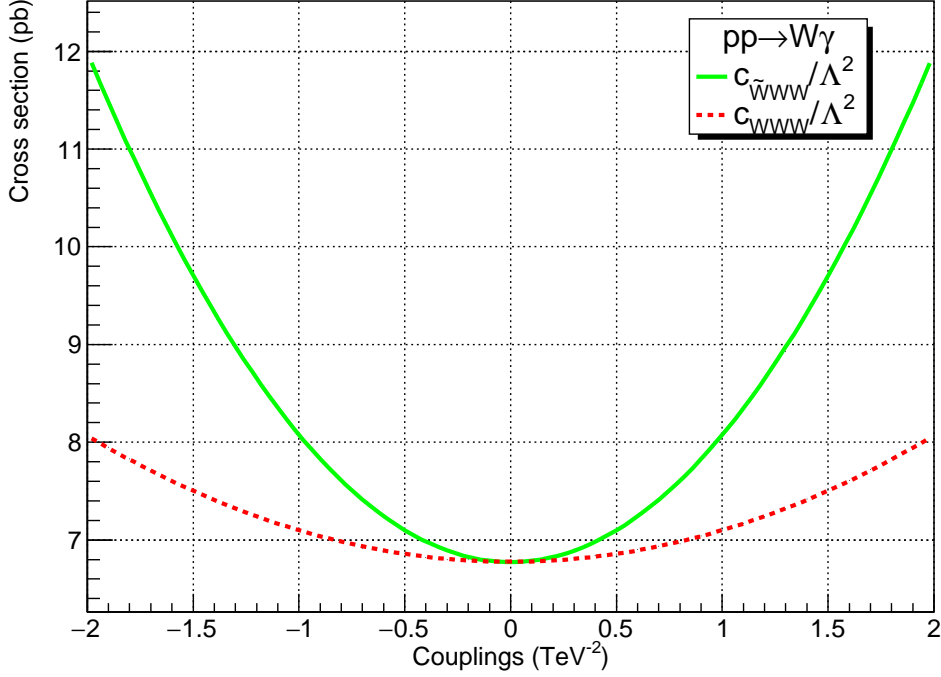


FIG. 3: The total cross-sections of the process $pp \rightarrow W^\pm \gamma$ as a function of the anomalous $C_{\tilde{W}WW}/\Lambda^2$ and C_{WWW}/Λ^2 couplings at the FCC-hh.

- $p_T^\gamma > 200$ GeV, $|\eta^\gamma| < 2.5$,
- MET > 40 GeV.

Production of $W^\pm \gamma$ events with photons having large transverse momentum p_T^γ is a sensitive search of new physics. The photon in the examined process has the advantage of being identifiable with high efficiency and purity. Also, as known, the high dimensional operators that define new physics parameters could affect the transverse momentum of the photon, particularly at high energy region of p_T^γ . This is very useful for distinguishing between signal and relevant backgrounds. The numbers of expected events as a function of p_T^γ photon transverse momentum for the $pp \rightarrow W^\pm \gamma$ signal and relevant backgrounds at the FCC-hh with $L_{int} = 3 \text{ ab}^{-1}$ and $\sqrt{s} = 100 \text{ TeV}$ are given in Fig. 4. We simulate signal ($pp \rightarrow W^\pm \gamma$) and interfering background ($pp \rightarrow W^\pm \gamma$) simultaneously, however other backgrounds are simulated separately. We have also used other coupling values in the signal simulation and in the analysis to produce the plots for estimated sensitivities as shown in Fig. 5 and Fig. 6.

TABLE II: Cross sections for the signal and the backgrounds in the relevant mode and decay channel at the FCC-hh.

Couplings (TeV ⁻²)	Mode	Decay Channel	Cross Section (pb)
$c_{WWW}/\Lambda^2 = 0.8$	$W^\pm + \gamma$	$l^\pm + \cancel{E_T} + \gamma$	9.6×10^{-1}
$C_{W,B}/\Lambda^2 = 40$	$W^\pm + \gamma$	$l^\pm + \cancel{E_T} + \gamma$	1.1×10^0
$c_{\tilde{W}WW}/\Lambda^2 = 0.4$	$W^\pm + \gamma$	$l^\pm + \cancel{E_T} + \gamma$	9.6×10^{-1}
$c_{\tilde{W}}/\Lambda^2 = 20$	$W^\pm + \gamma$	$l^\pm + \cancel{E_T} + \gamma$	1.0×10^0
Backgrounds	$W^\pm + \gamma$	$l^\pm + \cancel{E_T} + \gamma$	9.2×10^{-1}
	$W^\pm + j + \gamma$	$l^\pm + \cancel{E_T} + j + \gamma$	7.8×10^0
	$Z + \gamma$	$2l + \gamma$	2.9×10^{-1}
	$Z + j + \gamma$	$2l + j + \gamma$	6.0×10^{-1}
	$W^+ + W^- + \gamma$	$2l + \cancel{E_T} + \gamma$	5.3×10^{-3}
	$Z + Z + \gamma$	$2l + \cancel{E_T} + \gamma$	2.9×10^{-4}
	$W^\pm + j$	$l^\pm + \cancel{E_T} + j$	4.6×10^4
	$W^\pm + 2j + \gamma$	$l^\pm + \cancel{E_T} + 2j + \gamma$	1.2×10^1

III. EVALUATION OF RESULTS

In order to obtain sensitivity to the anomalous $C_{\tilde{W}}/\Lambda^2$, $C_{W,B}/\Lambda^2$, $C_{\tilde{W}WW}/\Lambda^2$ and C_{WWW}/Λ^2 couplings for the process $pp \rightarrow W^\pm \gamma$, we use a χ^2 method, where the χ^2 function with and without a systematic uncertainty is defined as follows

$$\chi^2 = \sum_i^{n_{bins}} \left(\frac{N_i^{NP} - N_i^B}{\Delta_i} \right)^2 \quad (25)$$

where N_i^{NP} is the total number of events in the existence of effective couplings, N_i^B is total number of events of the corresponding SM backgrounds in the i th bin of the p_T^γ distributions, $\Delta_i = \sqrt{\delta_{sys}^2 N_i^{B^2} + N_i^B}$ includes both the systematic (δ_{sys}) and statistical uncertainties in each bin.

The estimated sensitivities at 95% C.L. on the anomalous $C_{\tilde{W}}/\Lambda^2$, $C_{W,B}/\Lambda^2$, $C_{\tilde{W}WW}/\Lambda^2$ and C_{WWW}/Λ^2 couplings through the process $pp \rightarrow W^\pm \gamma$ at the FCC-hh with $\sqrt{s} = 100$ TeV, $L_{int} = 3 \text{ ab}^{-1}$, 30 ab^{-1} and no-sys, 5%, 10% are given in Tables III and IV. Also, in Figs.5 and 6, the achievable limits are shown as horizontal bar graphs. Our obtained 95%

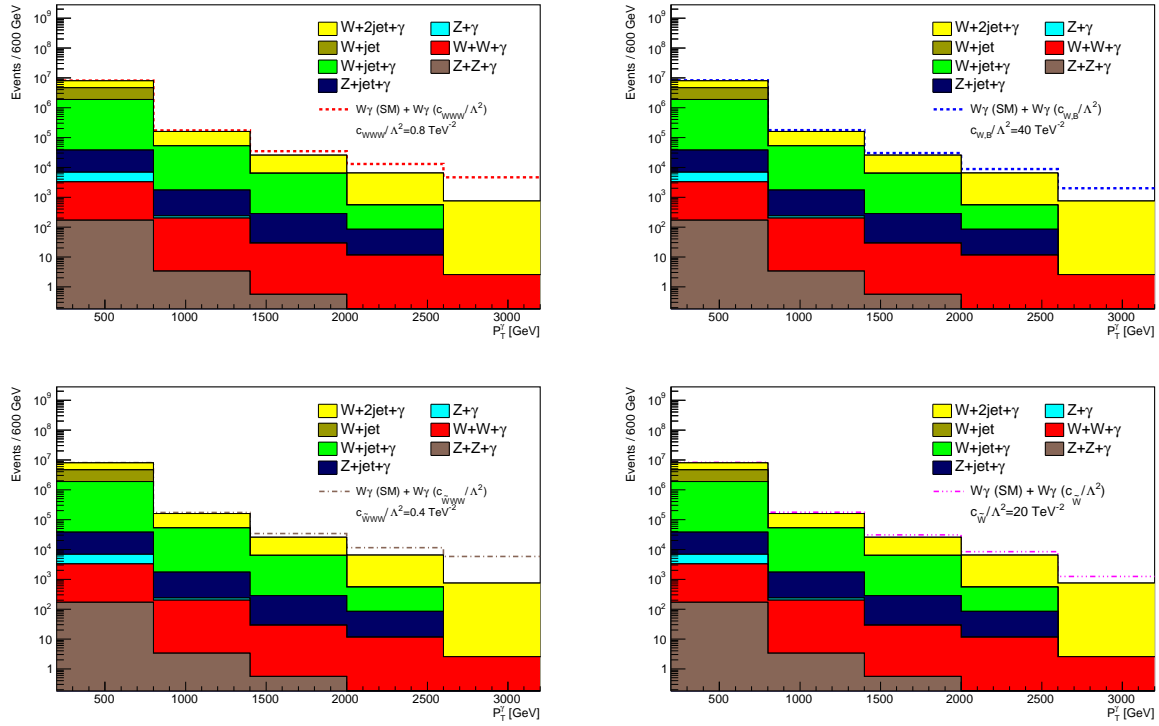


FIG. 4: The transverse momentum of the photon p_T^γ for the signals including certain values of the anomalous couplings and relevant backgrounds for the process $pp \rightarrow W^\pm \gamma$ at the FCC-hh. Here, the backgrounds are stack while the signal and interfering background are added (dashed lines).

C.L. limits without systematic uncertainties on the anomalous $C_{\tilde{W}}/\Lambda^2$, $C_{W,B}/\Lambda^2$, $C_{\tilde{W}WW}/\Lambda^2$ and C_{WWW}/Λ^2 couplings for the FCC-hh are $[-0.47; 0.47] \text{ TeV}^{-2}$, $[-0.88; 0.88] \text{ TeV}^{-2}$, $[-0.03; 0.03] \text{ TeV}^{-2}$ and $[-0.01; 0.01] \text{ TeV}^{-2}$, respectively.

TABLE III: Attainable limits on $C_{W,B}/\Lambda^2$ and $C_{\tilde{W}}/\Lambda^2$ couplings from dimension-6 operator at 95% C. L. for two different luminosity projections of 3 ab^{-1} and 30 ab^{-1} at the FCC-hh.

Couplings (TeV^{-2})	$L_{int} = 3 \text{ ab}^{-1}$			$L_{int} = 30 \text{ ab}^{-1}$		
	no-sys	5% sys	10% sys	no-sys	5% sys	10% sys
$C_{W,B}/\Lambda^2$	[-2.93; 2.69]	[-21.00; 19.75]	[-33.74; 28.11]	[-0.88; 0.88]	[-20.95; 19.28]	[-33.74; 28.11]
$C_{\tilde{W}}/\Lambda^2$	[-1.46; 1.50]	[-10.88; 11.18]	[-15.53; 15.50]	[-0.47; 0.47]	[-10.77; 11.06]	[-15.53; 15.50]

When we compare Table I, we see that we obtain better limits than current experimental limits. Here, C_{WWW}/Λ^2 coupling has the best sensitivity among the other couplings. For center-of-mass energy of 100 TeV with integrated luminosity 30 ab^{-1} , while we get the best

TABLE IV: Same as Table III but for C_{WWW}/Λ^2 and $C_{\tilde{W}WW}/\Lambda^2$ couplings.

Couplings (TeV^{-2})	$L_{int} = 3 \text{ ab}^{-1}$			$L_{int} = 30 \text{ ab}^{-1}$		
	no-sys	5% sys	10% sys	no-sys	5% sys	10% sys
C_{WWW}/Λ^2	[-0.03;0.03]	[-0.19;0.18]	[-0.35;0.34]	[-0.01;0.01]	[-0.18;0.17]	[-0.35;0.34]
$C_{\tilde{W}WW}/\Lambda^2$	[-0.05;0.04]	[-0.13;0.12]	[-0.17;0.16]	[-0.03;0.03]	[-0.13;0.12]	[-0.17;0.16]

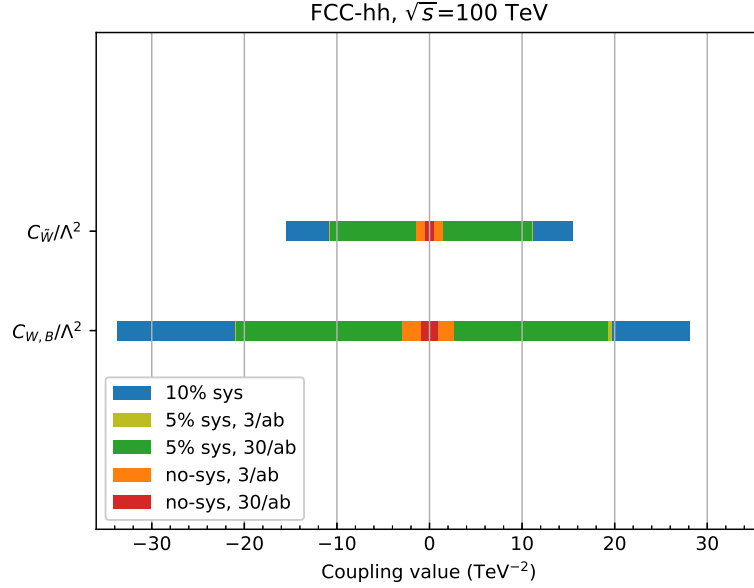


FIG. 5: The estimated sensitivities at 95% C.L. on the anomalous $C_{\tilde{W}}/\Lambda^2$ and $C_{W,B}/\Lambda^2$ couplings through the process $pp \rightarrow W^\pm \gamma$ at the FCC-hh with $\sqrt{s} = 100 \text{ TeV}$, $L_{int} = 3 \text{ ab}^{-1}$, 30 ab^{-1} and no-sys, 5% and 10%.

limits on the order of $O(10^{-1})$ for $C_{\tilde{W}}/\Lambda^2$, $C_{W,B}/\Lambda^2$ we obtain the limits on the order of $O(10^{-2})$ for $C_{\tilde{W}WW}/\Lambda^2$ and C_{WWW}/Λ^2 couplings in case of only statistical uncertainty. Also, our sensitivities obtained for $L_{int} = 30 \text{ ab}^{-1}$ without systematic uncertainty are almost up to 3 times better than derived $L_{int} = 3 \text{ ab}^{-1}$. For a systematic uncertainty of $\delta_{sys} = 10\%$, we estimate the sensitivities obtained on all couplings are better than the best experimental limit values. Also, our best limits on the anomalous couplings for $pp \rightarrow W^\pm \gamma$ with $\delta_{sys} = 5\%$ can be improved a factor of 1.5-2 according to the case with $\delta_{sys} = 10\%$. Figs.5 and 6 represent the limits on the anomalous couplings which do not increase proportionally to the increasing luminosity due to the systematic uncertainty considered here. The reason of this situation

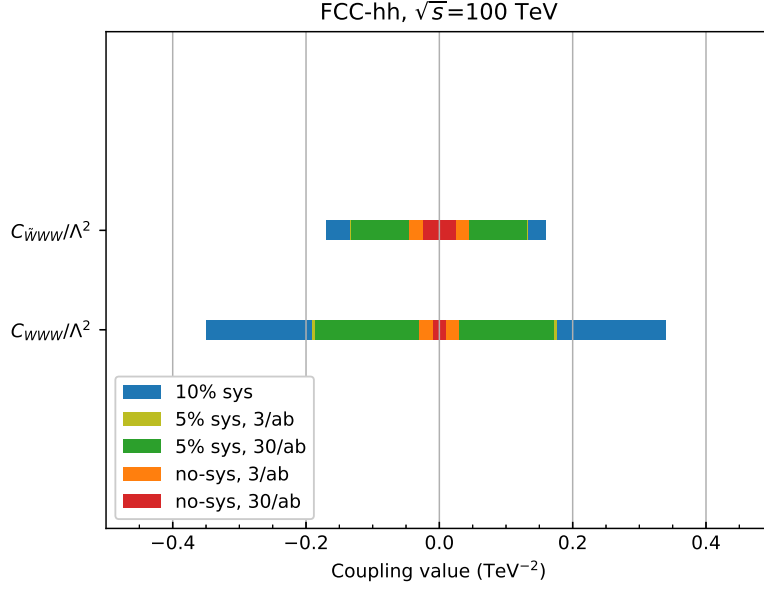


FIG. 6: Same as in Fig. 5 but for $C_{\tilde{W}WW}/\Lambda^2$ and C_{WWW}/Λ^2 .

is the systematic uncertainty which is much bigger than the statistical uncertainty. Thus, as can be seen Tables III-IV and Figs.5 and 6, if the systematic uncertainty is improved, we expect better limits on the anomalous couplings.

IV. CONCLUSIONS

We have examined the effects of dimension-6 operators giving rise to the anomalous interactions of $WW\gamma$ vertex through the process $pp \rightarrow W^\pm\gamma$ at the FCC-hh. The advantage of the process $pp \rightarrow W^\pm\gamma$ is that it studies the $WW\gamma$ couplings independently of WWZ effects. However, the high dimensional operators could affect p_T distribution of the photon in the final state, especially at the region with large p_T values, which can be very useful to distinguish signal and background events. Therefore, we use this as a tool to investigate the sensitivity to $C_{\tilde{W}}/\Lambda^2$, $C_{W,B}/\Lambda^2$, $C_{\tilde{W}WW}/\Lambda^2$ and C_{WWW}/Λ^2 couplings that are described by dimension-6 operators. Here, we suppose that only one anomalous couplings is non-zero at a time. We deduce that the FCC-hh collider will be able to provide sensitivity on the anomalous $WW\gamma$ couplings which can set more stringent limits by three (two) orders of magnitude with respect to the best sensitivities of $C_{\tilde{W}}/\Lambda^2$, $C_{W,B}/\Lambda^2$ ($C_{\tilde{W}WW}/\Lambda^2$ and C_{WWW}/Λ^2) couplings derived from CMS Collaboration for the process $pp \rightarrow W^\pm\gamma$ at the center-of-mass

energy of 13 TeV and integrated luminosity of 137 fb^{-1} [49]. We also discuss the impact of systematic uncertainties on our results. Including the systematic uncertainties increase the size of the estimated uncertainty and thus decrease the sensitivity on the anomalous couplings. As can be seen from Tables III and IV, our best limits obtained at $\delta_{sys} = 10\%$ systematic uncertainty are better than the current experimental limits [49]. As a result, we emphasize that the sensitivities obtained on the anomalous $WW\gamma$ couplings in this work are better than the sensitivity of the present experimental limits.

-
- [1] W. Buchmuller and D. Wyler, Nucl. Phys. B **268**, 621 (1986).
 - [2] S. Willenbrock and C. Zhang, Ann. Rev. Nucl. Part. Sci. **64**, 83 (2014).
 - [3] K. Hagiwara, S. Ishihara, R. Szalapski, and D. Zeppenfeld, Phys. Rev. D **48**, 2182 (1993).
 - [4] C. Degrande *et al.*, Annals Phys. **335**, 21 (2013).
 - [5] R. Li et al, Phys. Rev. D **97**, 075043 (2018).
 - [6] S. Tizchang and S. M. Etesami, JHEP **07**, 191 (2020).
 - [7] S. M. Etesami, S. Khatibi and M. M. Najafabadi, Eur. Phys. J. C **76**, 533 (2016).
 - [8] A. I. Ahmadov, Int. J. Theor. Phys. **58**, 2770 (2019).
 - [9] R. Li *et al.*, Phys. Rev. D **97**, 075043 (2018).
 - [10] U. Baur and D. Zeppenfeld, Phys. Lett. B **201**, 383 (1988).
 - [11] K. Hagiwara, R. D. Peccei, D. Zeppenfeld and K. Hikasa, Nucl. Phys. B **282**, 253-307 (1987).
 - [12] K. Hagiwara, S. Ishihara, R. Szalapski and D. Zeppenfeld, Phys. Lett. B **283**, 353-359 (1992).
 - [13] M. Wiest, D. R. Stump, D. O. Carlson and C. P. Yuan, Phys. Rev. D **52**, 2724-2736 (1995).
 - [14] M. Gintner, S. Godfrey and G. Couture, Phys. Rev. D **52**, 6249-6263 (1995).
 - [15] S. Ambrosanio and B. Mele, Nucl. Phys. B **374**, 3-35 (1992).
 - [16] İ. Şahin and A. A. Billur, Phys. Rev. D **83**, 035011 (2011).
 - [17] O. Kepka and C. Royon, Phys. Rev. D **78**, 073005 (2008).
 - [18] V. Arı, A. A. Billur, S. C. İnan and M. Köksal, Nucl. Phys. B **906**, 211-230 (2016).
 - [19] S. Atağ and İ. T. Çakır, Phys. Rev. D **63**, 033004 (2001).
 - [20] M. Köksal, A. A. Billur, A. Gutierrez-Rodriguez and M. A. Hernandez-Ruiz, Phys. Lett. B **808**, 135661 (2020).
 - [21] A. Gutierrez-Rodriguez, M. Köksal, A. A. Billur and M. A. Hernandez-Ruiz, J. Phys. G: Nucl. Part. Phys. **47**, 055005 (2020).
 - [22] S. Spor, A. A. Billur and M. Köksal, Eur. Phys. J. Plus **135**, 683 (2020).
 - [23] B. Şahin, Mod. Phys. Lett. A **32**, 1750205 (2017).
 - [24] L. Bian, J. Shu and Y. Zhang, Int. J. Mod. Phys. A **31**, 1644008 (2016).
 - [25] D. Choudhury and J. Kalinowski, Nuc. Phys. B **491**, 129-146 (1997).
 - [26] D. Choudhury, J. Kalinowski and A. Kulesza, Phys. Lett. B **457**, 193-201 (1999).
 - [27] S. Kumar and P. Poullose, Int. J. Mod. Phys. A **30**, 1550215 (2015).

- [28] A. Falkowski, M. G. Alonso, A. Greljo, D. Marzocca and M. Son, JHEP **02**, 115 (2017).
- [29] D. Bhatia, U. Maitra and S. Raychaudhuri, Phys. Rev. D **99**, 095017 (2019).
- [30] S. M. Etesami, S. Khatibi and M. M. Najafabadi, Eur. Phys. J. C **76**, 533 (2016).
- [31] I. T. Cakir, O. Cakir, A. Senol and A. T. Tasci, Acta Phys. Polon. B **45**, 1947 (2014).
- [32] B. Şahin, Phys. Scripta **79**, 065101 (2009).
- [33] S. Ataç and İ. Şahin, Phys. Rev. D **64**, 095002 (2001).
- [34] L. Bian, J. Shu and Y. Zhang, JHEP **09**, 206 (2015).
- [35] S. Schael *et al.* [ALEPH, DELPHI, L3, OPAL and LEP Electroweak Collaborations], Phys. Rept. **532**, 119-244 (2013).
- [36] G. Abbiendi *et al.* [OPAL Collaboration], Eur. Phys. J. C **19**, 229-240 (2001).
- [37] J. Abdallah *et al.* [DELPHI Collaboration], Eur. Phys. J. C **54**, 345-364 (2008).
- [38] T. Aaltonen *et al.* [CDF Collaboration], Phys. Rev. D **76**, 111103 (2007).
- [39] T. Aaltonen *et al.* [CDF Collaboration], Phys. Rev. Lett. **102**, 242001 (2009).
- [40] T. Aaltonen *et al.* [CDF Collaboration], Phys. Rev. Lett. **104**, 201801 (2010).
- [41] V. M. Abazov *et al.* [D0 Collaboration], Phys. Lett. B **718**, 451-459 (2012).
- [42] S. Chatrchyan *et al.* [CMS Collaboration], Eur. Phys. J. C **73**, 2610 (2013).
- [43] M. Aaboud *et al.* [ATLAS Collaboration], Eur. Phys. J. C **77**, 563 (2017).
- [44] A. M. Sirunyan *et al.* [CMS Collaboration], Eur. Phys. J. C **76**, 401 (2016).
- [45] A. M. Sirunyan *et al.* [CMS Collaboration], JHEP **12**, 062 (2019).
- [46] R. Li *et al.*, Phys. Rev. D **97**, 075043 (2018).
- [47] A. A. Billur, M. Koksall, A. Gutierrez-Rodriguez, M. A. Hernandez-Ruiz, Eur. Phys. J. Plus **136**, 697 (2021).
- [48] L. Bian, J. Shu, Y. Zhang, Int. J. Mod. Phys. A **31**, 1644008 (2016).
- [49] A. M. Sirunyan *et al.* [CMS Collaboration], Phys. Rev. Lett. **126**, 252002 (2021).
- [50] A. Abada, *et al.* [FCC Collaboration], Eur. Phys. J. Spec. Top. **228**, 755 (2019).
- [51] J. Alwall, *et al.* JHEP **1407**, 079 (2014).
- [52] A. Alloul, *et al.* Comput. Phys. Commun. **185**, 2250 (2014).
- [53] C. Degrande, *et al.* Comput. Phys. Commun. **183**, 1201 (2012).
- [54] T. Sjostrand, *et al.* Comput. Phys. Commun. **191**, 159 (2015).
- [55] J. de Favereau, *et al.* JHEP, 1402, 057, (2014).
- [56] <http://madgraph.hep.uiuc.edu/Downloads/ExRootAnalysis>.

- [57] R. Brun and F. Rademakers, Nuclear Instruments and Methods in Physics Research Section A: Accelerators, Spectrometers, Detectors and Associated Equipment, 389, 81, (1997).